

- Goodridge, F., and I. D. Robb, "Mechanism of Interfacial Resistance in Gas Absorption," *I&EC Fund.*, 4, 49 (1965).
- Harvey, E. Q., and W. Smith, "The Absorption of Carbon Dioxide by a Quiescent Liquid," *Chem. Eng. Sci.*, 10, 274 (1959).
- Haq, M. A., "Fluid Dynamics on Sieve Trays," *Hydroc. Processing*, 61(4), 165 (1982).
- Hikita, H., S. Asai, and T. Takatsuka, "Absorption of Carbon Dioxide into Aqueous Sodium Hydroxide and Sodium Carbonate-Bicarbonate Solutions," *Chem. Eng. J.*, 11, 131 (1976).
- Hoffer, M. S., and E. Rubin, "Flow Regimes of Stable Foams," *I&EC Fund.*, 8, 483 (1969).
- Johansson, G., and S. Brander, "Reactive Foams for Air Purification," Fifth Int. Cong. on Chem. Eng., Copenhagen (Apr., 1980).
- Kaldor, T. G., and C. R. Phillips, "Aerosol Scrubbing by Foam," *I&EC Process Des. Dev.*, 15, 1 (1976).
- Kolthoff, I. M., and E. B. Sandler, *Textbook of Quantitative Inorganic Analysis*, 3rd Ed., MacMillan Co., New York, 531 (1952).
- Metzner, A. B., and L. F. Brown, "Mass Transfer in Foams," *Ind. Eng. Chem.*, 48, 2040 (1956).
- Nguyen Ly, L. A., R. G. Carbonell, and B. J. McCoy, "Diffusion of Gases Through Surfactant Films: Interfacial Resistance to Mass Transfer," *AIChE J.*, 25, 1015 (1979).
- Plevan, R. E., and J. A. Quinn, "The Effect of Monomolecular Films on the Rate of Gas Absorption into a Quiescent Liquid," *AIChE J.*, 12, 894 (1966).
- Sherwood, T. K., R. L. Pigford, and C. R. Wilke, *Mass Transfer*, McGraw-Hill, New York (1975).
- Springer, T. K., and R. L. Pigford, "Influence of Surface Turbulence and Surfactants on Gas Transport Through Liquid Interfaces," *I&EC Fund.*, 9, 458 (1970).
- Thompson, D. W., "Effect of Interfacial Mobility on Mass Transfer in Gas-Liquid Systems," *I&EC Fund.*, 9, 243 (1970).
- Whitaker, S., and R. L. Pigford, "Response of a Gas-Liquid Interface to Concentration Pulses," *AIChE J.*, 741 (1966).

Manuscript received May 20, 1983; revision received September 15, and accepted September 26, 1983.

# Analysis of Staged Liquid Surfactant Membrane Operations

Graphical and numerical procedures are presented for the design and analysis of cocurrent and countercurrent multistaged mixer-settler units for liquid membrane extraction operations—these are based on the recently developed Advancing Front Model of Ho et al. (1982) and Hatton et al. (1983). The numerical results indicate that the extraction efficiency in a countercurrent cascade is only slightly improved over that for cocurrent operation. However, for any given stage, marked improvements in extraction efficiency are indicated if an external emulsion recycle over the mixer settler unit is used to ensure adequate holdup ratios in the mixer. Premixing of the emulsion feed and recycle streams will impair the extraction performance, however,

T. A. HATTON and  
D. S. WARDIUS

Department of Chemical Engineering  
Massachusetts Institute of Technology  
Cambridge, MA 02139

## SCOPE

Despite a continuing strong interest in liquid surfactant membrane operations, very little attention has been devoted to discussion of scale-up and design procedures for these processes. In the one paper addressing this problem directly, it was suggested that the model of Cahn and Li (1974) be used for the sizing of continuous, multistage processing equipment. However, their implicit assumption of an unchanging resistance to mass transfer during extraction could not be substantiated by their experimental findings, nor by those of subsequent workers (Hochhauser and Cussler, 1975; Kondo et al., 1979; Hatton et al., 1983). In an attempt to improve the predictive value of these process models, Ho et al. (1982) and Hatton et al. (1983) developed the so-called Advancing Front Model for batch and con-

tinuous operations, respectively, in which cognizance was taken of the increase in mass transfer resistance with increasing contact time. They found that the model provided a very good description of the mass transfer processes occurring during their solute extraction experiments. Their results bode well for the effective implementation of this model in the design and analysis of multistage, liquid membrane extraction operations, and the purpose of this paper is to extend the earlier developments for single-stage, continuous extraction processes (Hatton et al., 1983) to allow also for the analysis and design of cocurrent and countercurrent multistage operations in terms of the Advancing Front Model.

## CONCLUSIONS AND SIGNIFICANCE

Liquid surfactant membrane extraction operations are well described by the Advancing Front Model; the model assumes that an instantaneous and irreversible reaction between the diffusing solute and the immobile internal reagent occurs at a reaction front which moves into the emulsion globule as the

reaction proceeds. Based on this model, a simple graphical procedure has been developed for the design and analysis of cocurrent and countercurrent multistaged liquid membrane operations. The results indicate an increase in extraction efficiency when the countercurrent rather than the cocurrent arrangement is used, although the differences in overall fractional utilization of internal reagent for the two cases are slight, being

Correspondence concerning this paper should be addressed to T. A. Hatton.

at most about 5%. Also, it is apparent that the incorporation of a recycle stream over a mixer-settler unit will improve dramatically the extraction efficiency of the system, other factors being equal. However, some differences in performance are noted if the recycle stream is premixed with the emulsion feed instead

of being introduced separately to the mixer. Both observations relate directly to the manner in which diffusional resistances to mass transfer develop within a globule, and this in turn is affected strongly by the initial internal reagent concentration within the individual globules of emulsion.

## INTRODUCTION

Liquid surfactant membranes provide a potentially powerful technique for effecting a diverse number of separations operations, while simultaneously allowing the extracted solute to be concentrated strongly in the receiving phase. These membrane systems, Figure 1, consist of an emulsion dispersed in the continuous feed solution as globules of approximately 0.1–2 mm in diameter. Solute extracted by the emulsion diffuses into the globules and is trapped by reaction with an internal reagent encapsulated in the drops making up the dispersed phase of the emulsion. These drops have diameters of 1–10  $\mu\text{m}$ . The effluent emulsion is subsequently broken to enable collection of the concentrated solution in the encapsulated droplets. The liquid membrane separating the feed solution from the aqueous internal phase droplets usually consists of a specially formulated oil phase containing various additives to ensure adequate membrane strength and high selectivity for the solute to be extracted.

The most frequent applications of these liquid membrane systems have been in the extraction of heavy metal ions (Schiffer et al., 1974; Hochhauser and Cussler, 1975; Martin and Davies, 1976/1977; Kondo et al., 1979, 1981; Völkel et al., 1980; Strezelbicki and Charewicz, 1980; Schlosser and Kossaczky, 1980; Frankenfeld et al., 1981; Bock et al., 1981; Hayworth et al., 1982; Bock and Valint, 1982) and in the removal of trace contaminants from waste water (Li and Shrier, 1972; Cahn and Li, 1974; Matulevicius and Li, 1975; Frankenfeld and Li, 1977; Kitagawa et al., 1977; Cahn et al., 1978; Halwachs et al., 1980; Schlosser and Kossaczky, 1980; Terry et al., 1982; Ho et al., 1982; Hatton et al., 1983). Hydrocarbons may also be fractionated using an aqueous membrane phase to encapsulate an organic mixture in the emulsion droplets and then dispersing this emulsion in an organic receiving phase (Li, 1971a, 1971b; Shah and Owens, 1972; Cahn and Li, 1976a, 1976b; Alessi et al., 1980; Halwachs et al., 1980; Schlosser and Kossaczky, 1980; Kremesec and Slatery, 1982). Other applications have been found in the biochemical and biomedical fields, and include the works of May and Li (1972, 1974, 1977), Li and Asher (1973), Mohan and

Li (1974, 1975), Asher et al. (1975, 1977) and Frankenfeld et al. (1978).

To date, the only consideration that has been given to the design of multistage mixer-settler systems for liquid membrane (LM) processes is the work of Cahn and Li (1974). They assumed that the rate of solute uptake by the membrane emulsion could be described by

$$r_o = \text{rate per unit volume} = D' \phi_e \Delta c$$

where  $D'$  is the so-called permeation rate constant, and the holdup ratio  $\phi_e = V_E/V_W$  was obtained in the belief that the area available for mass transfer is proportional to this quantity. This model essentially assumes that all resistance to diffusion lies within a thin membrane film of constant thickness surrounding the trapped internal reagent phase, and has been used in various forms by many other authors (Hatton et al., 1982). In most LM applications, the concentration of the permeating solute in the receiving phase can be taken to be zero, since there it is removed by reaction with the internal reagent. Hence the concentration driving force  $\Delta c$  is merely the permeate concentration  $c$  in the external, continuous phase. Cahn and Li (1974) suggested that the permeation rate constants  $D'$  be estimated from batch extraction runs using the integrated rate equation

$$\ln \frac{c_0}{c} = D' \phi_e t, \quad (2)$$

and that they then be employed in the design of continuous, multistage mixers. For an  $N$ -stage system, each stage being of equal volume, the appropriate volume per mixer would be

$$V_M = K \left( \sqrt[N]{\frac{c_0}{c_1}} - 1 \right) \quad (3)$$

where

$$K = \frac{v_W}{D'} (1 + 1/\phi_e), \quad (4)$$

$c_0$  and  $c_1$  are the feed and desired effluent concentrations, respectively, and  $v_W$  is the water-phase flow rate.

While this approach has in its favor its direct simplicity, there are nevertheless certain drawbacks to its use. It has been found experimentally that the values of  $D'$  or, equivalently, the membrane film thickness, estimated using Eq. 2 vary depending on the specific time interval employed in their determination (Cahn and Li, 1974; Hochhauser and Cussler, 1975; Kondo et al., 1979). Moreover, it is not clear that the coefficients thus determined are even appropriate for application in the design of continuous extraction operations. For instance, Hatton et al. (1983) found that  $D'$  is a strong function of the fractional utilization of the internal reagent; hence it should be expected to vary from one stage to the next, contrary to the assumptions inherent in the design Eq. 3. This variation in  $D'$  was interpreted in terms of a more detailed mathematical description of the LM transport processes—the Advancing Front Model—wherein the encapsulated internal reagent droplets were treated as immobile solute sinks of finite capacity interacting with the surrounding membrane phase through which the solute diffuses. The success of this model in correctly predicting LM mass transfer behavior suggests that it would be more suitable for design purposes than any model based on the permeation rate constant  $D'$ . This view is reinforced by the excellent agreement found between experimental batch extraction runs and the predictions afforded by the Advancing Front Model recently presented by Ho et al. (1982). A similar modelling approach has also been successful

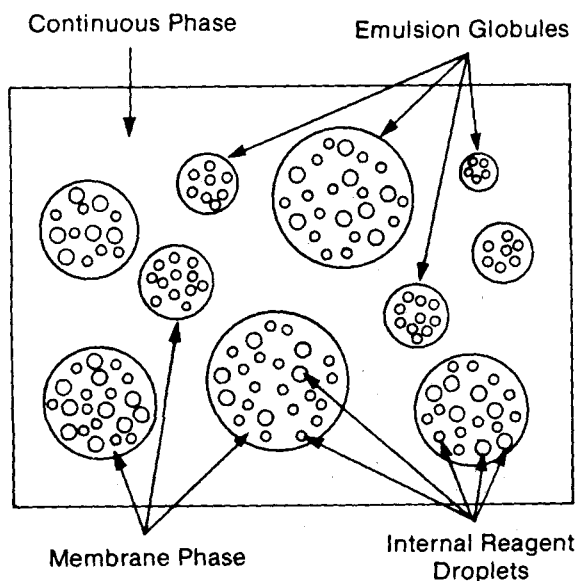


Figure 1. Liquid surfactant membrane system.

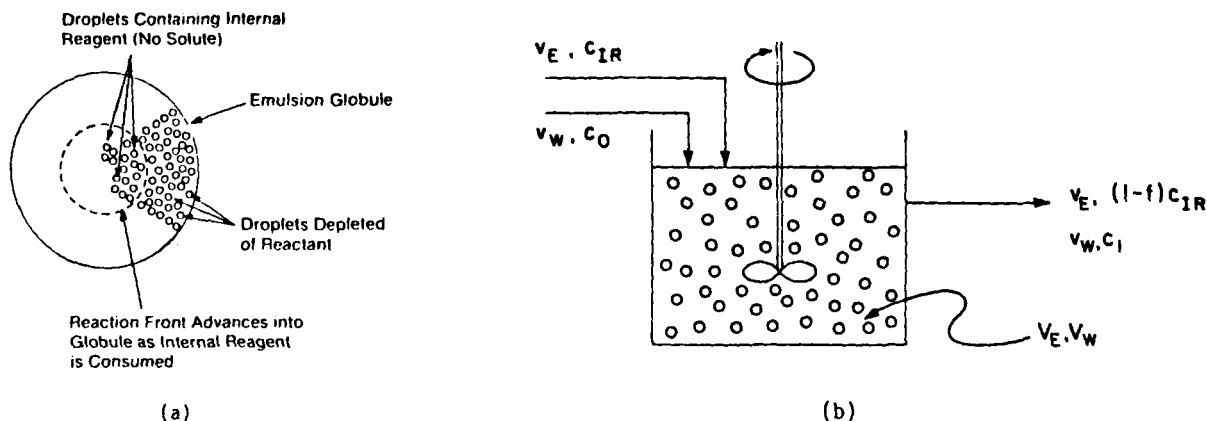


Figure 2. The Advancing Front Model: (a) Individual globule (b) continuous mixer unit.

in correlating the batch experimental data of Kopp et al. (1978) and Teramoto et al. (1981).

With these observations in mind, we have extended our earlier results on the Advancing Front Model to show how it can be employed effectively in the design of multistage mixer-settler systems for liquid membrane operations. A simple graphical procedure, easily implemented for direct computer calculations, has been developed for this purpose, and is described in the subsequent sections of this paper. We also address the problem of the effect of an external recycle stream over an individual stage in a mixer-settler train on the extraction efficiency of the mixer concerned.

#### THE ADVANCING FRONT MODEL

In the development of a tractable physical model for solute transport and chemical reaction in a typical liquid membrane system, care should be taken to account realistically for the heterogeneous nature of the emulsion globules. It is also important that the solute interactions between the encapsulated internal reagent drops and the surrounding membrane phase be handled in a physically realistic manner, as should be the interactions between the emulsion globules themselves and the external, continuous phase. Ho et al. (1982) have discussed in some detail the development of a model meeting these requirements, justifying on physical grounds each assumption made in their analysis. The model details are summarized here.

It is assumed that all emulsion globules in the system are uniform in size, nonoscillating and stagnant, and that mass transfer within the globules is by diffusion only. Coalescence of the globules is assumed to be negligible. The emulsion itself can be treated as a continuum and the encapsulated internal reagent is considered to be a uniformly distributed and immobile species within the continuum. Reactions between the reagent and the diffusing solute are assumed to be instantaneous and irreversible. Hence the solute is unable to penetrate into the globule beyond those droplets which are completely depleted of reagent, for it is then immediately removed by reaction with the internal reagent. Consequently, a sharp "reaction front" must develop, separating a region containing only reaction products, and no reagent, from an inner, core region containing only unreacted internal reagent, but no solute. This reaction front advances in towards the globule centre as the internal reagent is consumed by the reaction, Figure 2. In general, the reaction products are insoluble in the membrane phase, and the reacted solute is therefore trapped in the encapsulated drops.

The external phase is considered to be sufficiently well agitated that external mass transfer resistances at the globule surface can be assumed to be negligible. Moreover, for well-mixed, continuous reactors the globule residence time distribution will be exponential;

if  $n(t)$  is the fraction of globules having residence time greater than  $t$ , then

$$n(t) = e^{-t/T} \quad (5)$$

Here  $T = V_E/v_E$  is the average residence time of the emulsion in the mixer.

With this set of assumptions, the equation describing the solute transport in an emulsion globule is

$$\frac{\partial c_g}{\partial t} = \frac{\mathcal{D}}{r^2} \frac{\partial}{\partial r} \left( r^2 \frac{\partial c_g}{\partial r} \right) \quad (6)$$

with the initial condition

$$\text{at } t = 0 \quad c_g = 0 \quad (7)$$

and boundary conditions

$$\text{at } r = R \quad c_g = \alpha c_1 \quad (8)$$

$$\text{at } r = R_f(t) \quad c_g = 0 \quad (9)$$

Here  $c_g$  is the solute concentration in the emulsion averaged locally over both the membrane and the encapsulated droplet phases, and  $\mathcal{D}$  is an effective diffusion coefficient for the solute in the emulsion. The globule radius is  $R$ , the position of the advancing reaction front is  $R_f(t)$ , the external, continuous phase concentration is  $c_1$ , and  $\alpha$  is the partition coefficient for the solute between the external phase and the emulsion. A material balance over the reaction front yields

$$\frac{dR_f}{dt} = - \frac{\mathcal{D}}{c_{IR}} \frac{\partial c_g}{\partial r} \bigg|_{r=R_f} \quad (10)$$

with initial condition

$$\text{at } t = 0 \quad R_f = R \quad (11)$$

The concentration of the internal reagent per unit volume of emulsion is  $c_{IR}$ .

On defining the dimensionless variables

$$\tau = \frac{\epsilon \mathcal{D} t}{R^2} \quad \eta = \frac{r}{R} \quad \chi = \frac{R_f}{R}$$

$$g = \frac{c_g}{\alpha c_1} \quad \epsilon = \frac{\alpha c_1}{c_{IR}}$$

Equations 6 through 11 reduce to

$$\epsilon \frac{\partial g}{\partial \tau} = \frac{1}{\eta^2} \frac{\partial}{\partial \eta} \left( \eta^2 \frac{\partial g}{\partial \eta} \right) \quad (12)$$

$$\tau = 0 \quad g = 0 \quad (13)$$

$$\eta = 1 \quad g = 1 \quad (14)$$

$$\eta = \chi \quad g = 0 \quad (15)$$

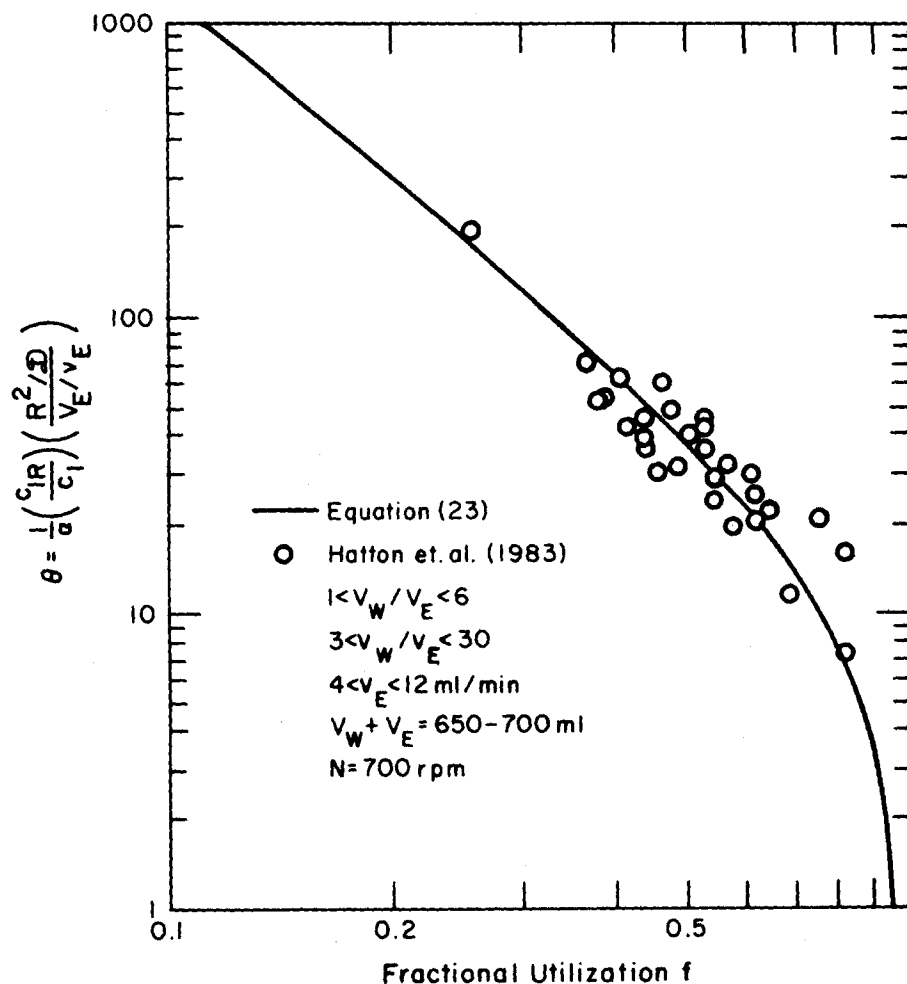


Figure 3. Performance curve for continuous liquid surfactant membrane operations.

$$\frac{d\chi}{d\tau} = -\frac{\partial g}{\partial \eta} \bigg|_{\eta=\chi} \quad (16)$$

$$\tau = 0 \quad \chi = 1 \quad (17)$$

This system of equations is nonlinear, and has been solved by Pedrosa and Domoto (1973) using perturbation methods. For  $\epsilon$  small, as it usually is for cases of interest in liquid membrane separations, it is sufficient to retain only the zero-order solution, corresponding to the pseudo steady state assumption. Thus,

$$g = \frac{1}{\eta} \left( \frac{\eta - \chi}{1 - \chi} \right) \quad (18)$$

$$\tau = \frac{1}{6} (1 - 3\chi^2 + 2\chi^3) \quad (19)$$

Now, a material balance over the mixer yields

$$\begin{aligned} v_W(c_0 - c_1) &= N_T \int_0^1 4\pi R^2 \mathcal{D} \frac{\partial c_E}{\partial r} \bigg|_{r=R} dn(t) \\ &= \frac{N_T}{T} \int_0^\infty 4\pi R^2 \mathcal{D} \frac{\partial c_E}{\partial r} \bigg|_{r=R} e^{-t/T} dt \quad (20) \end{aligned}$$

where the overall mass transfer rate in the system has been obtained by integrating the individual rates over all the globules in the mixer, allowing for their exponential residence time distribution. Note that  $N_T = V_E/(4\pi R^3/3)$  is the total number of globules in the system.

Equation 20 can be rearranged to give

$$f = \frac{v_W(c_0 - c_1)}{v_E c_{IR}} = 3 \int_0^\infty \frac{\partial g}{\partial \eta} \bigg|_{\eta=1} e^{-\theta \tau} d\tau \quad (21)$$

where

$$\theta = \left( \frac{c_{IR}}{c_1} \right) \frac{R^2/\alpha \mathcal{D}}{V_E/v_E} \quad (22)$$

and  $f$  represents the fractional utilization of the internal reagent. Using Eqs. 18 and 19, Eq. 21 can be expressed as

$$f = 3 \int_0^1 \chi^2 \exp \left[ -\frac{\theta}{6} (1 - 3\chi^2 + 2\chi^3) \right] d\chi \quad (23)$$

where the variable of integration has been changed from  $\tau$  to  $\chi$ .

The result (23) indicates that the fractional utilization  $f$  can be uniquely related to the parameter  $\theta$ , and this relation is shown graphically in Figure 3. Also shown are the experimental results of Hatton et al. (1983) obtained for the extraction of ammonia from simulated waste water using a 3%  $H_2SO_4$  solution as the internal reagent phase. In plotting these data, the diffusion response time,  $R^2/\alpha \mathcal{D}$ , was treated as an adjustable parameter, since globule sizes were not determined during the experimental runs. A value of about 30 min. for this response time was found to give favorable agreement between the experimental data and the theoretical predictions, as is evident from Figure 3. This value is of the expected order of magnitude, and thus the results presented here give strong support for the validity of the Advancing Front model in the description of liquid membrane operations, particularly when it is noted that these data were gathered over a wide range of operating conditions. Based on these conclusions, we feel justified in extending our analysis to the other, more complex extraction configurations considered in the next few sections.

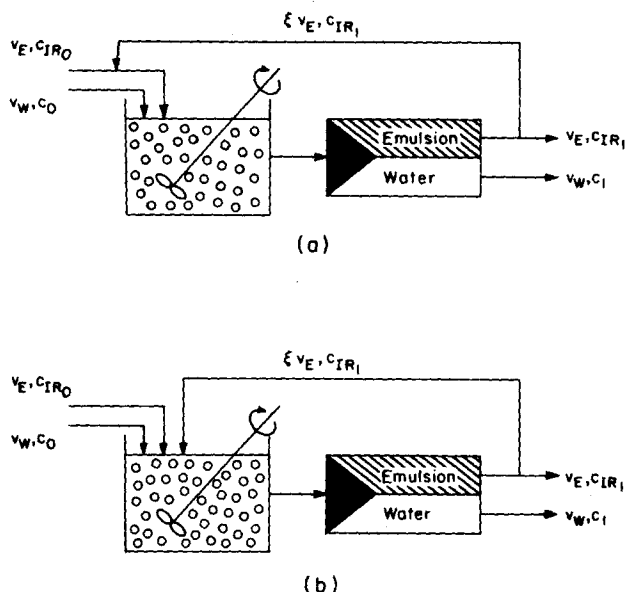


Figure 4. Mixer-settler units with emulsion recycle: (a) premixed and (b) non-premixed emulsion feed and recycle.

### EFFECT OF AN EXTERNAL RECYCLE

Mass transfer considerations frequently require an emulsion-to-feed holdup ratio in the mixer,  $V_E/V_W$ , significantly different from the stoichiometrically-determined ratio of feed rates to the mixer,  $v_E/v_W$ . Traditionally, the desired holdup ratio has been attained by recycling a portion of the effluent emulsion from the settler back to the mixer, as shown in Figure 4. This has the effect of reducing the average internal reagent (IR) concentration of the emulsion introduced to the mixer. Since the overall solute extraction rate depends on this initial IR concentration in a nonlinear fashion, as reflected in the  $\theta$  vs.  $f$  relationship of the preceding section, it is to be anticipated that the performance characteristics of the unit will be sensitive to whether the recycle and emulsion feed streams are mixed before being fed to the mixer, or whether they are introduced separately. Figures 4a and 4b depict the two process configurations. In the first case (case (a)), the internal reagent concentration will be the same for all globules fed to the system, and will be the average  $c_{IR}$  value for the emulsion feed and recycle streams. In case (b), however, there will be two classes of globules, those having an initial IR concentration corresponding to that of the feed, and those with an initial reagent concentration corresponding to the average effluent IR concentration. We investigate the performance characteristics of both configurations below.

There is a third configuration whereby the holdup ratio can be enhanced independently of the feed rates, and this is the internal recycle mixer proposed by Hatton et al. (1983), which circumvents the need for the introduction of an external recycle stream. In this device the globules retain their identities during their stay in the mixer, and there is no internal mixing of the globule contents. The analysis given in the preceding section pertains directly to this case.

### Premixed Emulsion Feed and Recycle

This scheme is illustrated in Figure 4a, and we consider balances both over the entire stage and over the mixer itself. We use primed quantities  $f'$  and  $\theta'$  to denote conditions in the mixer, and, as before,  $f$  and  $\theta$  refer to the performance of the entire stage.

The averaged internal reagent concentration of the combined emulsion feed and recycle streams is

$$c'_{IR} = \left[ \frac{1 + (1-f)\xi}{1 + \xi} \right] c_{IR0} \quad (24)$$

and, using the results obtained previously, it follows that the fractional utilization of internal reagent over the mixer itself is

$$f' = \frac{v_W(c_0 - c_1)}{v_E(1 + \xi)c'_{IR}} = 3 \int_0^1 \chi^2 \exp \left[ -\frac{\theta'}{6}(1 - 3\chi^2 + 2\chi^3) \right] d\chi \quad (25)$$

where

$$\theta' = \left( \frac{c'_{IR}}{c_1} \right) \frac{R^2/\alpha D}{V_E/v_E(1 + \xi)} = [1 + (1-f)\xi]\theta \quad (26)$$

and  $f$  and  $\theta$  are as defined earlier. It is then readily shown that

$$\frac{f}{1 + (1-f)\xi} = 3 \int_0^1 \chi^2 \exp[-(1 + (1-f)\xi)\theta] \times \frac{\theta}{6}(1 - 3\chi^2 + 2\chi^3) d\chi \quad (27)$$

which gives  $f$  implicitly as a function of  $\xi$  and  $\theta$ . For  $\xi = 0$ , Eq. 22 is recovered.

### Nonpremixed Emulsion Feed and Recycle

In this case, illustrated schematically in Figure 4b, the globules derived from the two streams must be considered separately and the fractional utilization of internal reagent over the mixer,  $f'$ , will be a weighted average of the  $f$ -values for the two classes of globules i.e.

$$f' = \frac{1}{(1 + \xi)} [f'_F + \xi f'_R] \quad (28)$$

where  $f'_F$  and  $f'_R$  are the fractional utilizations of internal reagent in the feed and recycle streams, respectively. Again, the results obtained for the no-recycle case can be adapted directly, and we obtain

$$f' = \frac{1}{(1 + \xi)} \left[ 3 \int_0^1 \chi^2 \exp \left[ -\frac{\theta'_F}{6}(1 - 3\chi^2 + 2\chi^3) \right] d\chi + 3\xi \int_0^1 \chi^2 \exp \left[ -\frac{\theta'_R}{6}(1 - 3\chi^2 + 2\chi^3) \right] d\chi \right] \quad (29)$$

where

$$\theta'_F = \left( \frac{c_{IR0}}{c_1} \right) \frac{R^2/\alpha D}{V_E \left( \frac{1}{1 + \xi} \right) / v_E} = (1 + \xi)\theta \quad (30)$$

and

$$\theta'_R = \left( \frac{c_{IR1}}{c_1} \right) \frac{R^2/\alpha D}{V_E \left( \frac{\xi}{1 + \xi} \right) / \xi v_E} = (1 + \xi)(1 - f)\theta \quad (31)$$

note being taken of the relation  $c_{IR1} = (1 - f)c_{IR0}$ . Also, since

$$f' = \frac{v_W(c_0 - c_1)}{v_E[c_{IR0} + \xi c_{IR1}]} \quad (32)$$

it is readily shown that Eq. 29 is equivalent to

$$\frac{f}{1 + (1-f)\xi} = \frac{3}{(1 + \xi)} \times \left[ \int_0^1 \chi^2 \exp \left[ -(1 + \xi)\frac{\theta}{6}(1 - 3\chi^2 + 2\chi^3) \right] d\chi + \xi \int_0^1 \chi^2 \exp \left[ -(1 + \xi)(1 - f)\frac{\theta}{6}(1 - 3\chi^2 + 2\chi^3) \right] d\chi \right] \quad (33)$$

from which  $f$  can be obtained as a function of the parameters  $\xi$  and  $\theta$ .

### Comparison of Recycle Premixing Policies

The effect of a recycle stream on the performance of a single mixer-settler unit is illustrated in Figure 5, where the results are given as  $\theta$  vs.  $f$  with the recycle ratio  $\xi$  as parameter. The broken lines are the results obtained from premixed feed and recycle streams (case a), while the solid curves give the behaviour in the

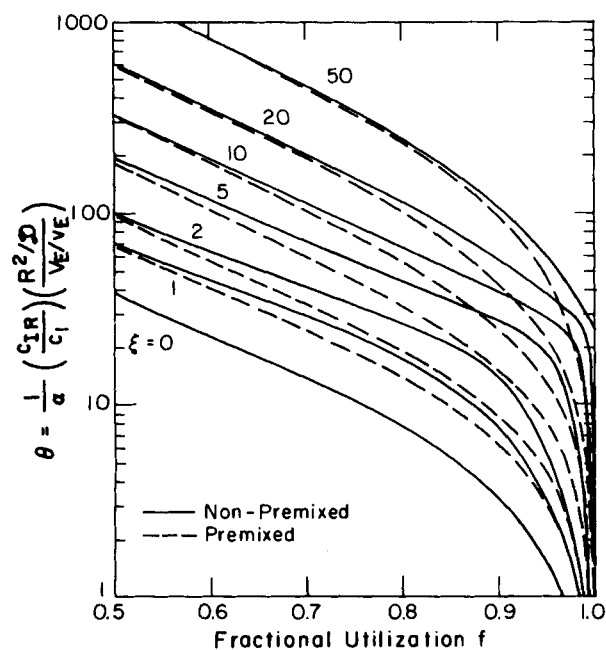


Figure 5. Effect of recycle and premixing policies on performance of a mixer-settler unit.

absence of premixing (case *b*). Clearly, the separate introduction of the emulsion feed and recycle streams to the mixer will yield a performance somewhat improved over that obtained when these streams are premixed. This is primarily due to the nonlinear nature of the extraction processes, and is related to the relative rates at which the reaction front penetrates the emulsion globules depending on their initial internal reagent concentrations.

The extent of the improvement in performance when there is no premixing is perhaps best illustrated by comparing the relative volumes of the mixers required to perform a given separations task using the two recycle configurations considered here. Shown on Figure 6 is the ratio  $\theta_a/\theta_b$  as a function of  $f$  with  $\xi$  as parameter, where the subscripts *a* and *b* refer to the premixed (case *a*) and nonpremixed (case *b*) arrangements, respectively. If the concentrations, flow rates and holdup ratios are the same in two cases, then it is readily shown that  $\theta_a/\theta_b = V_b/V_a$ , where  $V_a$  and  $V_b$  are the mixer volumes required for cases *a* and *b*, respectively.

On inspection of the curves given in Figure 6, it is evident that for the lower values of the fractional utilization  $f$ , an increase in the recycle ratio  $\xi$  will reduce the effect of premixing on the mixer volume requirements. However, as  $f$  increases, the trend is reversed, and increasing  $\xi$  leads to a much greater discrepancy in the volume requirements for the two cases. It must be remarked, though, that the fractional utilizations for which these large differences in mixer volumes arise are beyond the range of  $f$  values normally encountered in practice. Moreover, for values of  $f$  of practical interest ( $f < 0.7$ , say), the maximum differences in mixer volume requirements are less than 20%. We can therefore conclude that while the separate introduction of the two emulsion streams to the mixer is desirable, it is not imperative, and adequate performance can be obtained if the streams are premixed.

## MULTISTAGE MIXER-SETTLER SYSTEMS

The results presented above will be applicable to any single stage in a mixer-settler train, provided the feed and effluent concentrations used in the definition of  $\theta$  are correctly identified, and that the emulsion feed to the given stage is of a uniform internal reagent concentration. This latter condition will be obtained when inter-stage settling is permitted. Moreover,  $f$  will now refer to the fractional utilization of the internal reagent that is fed to the stage; it does *not* represent the overall utilization up to that point of the

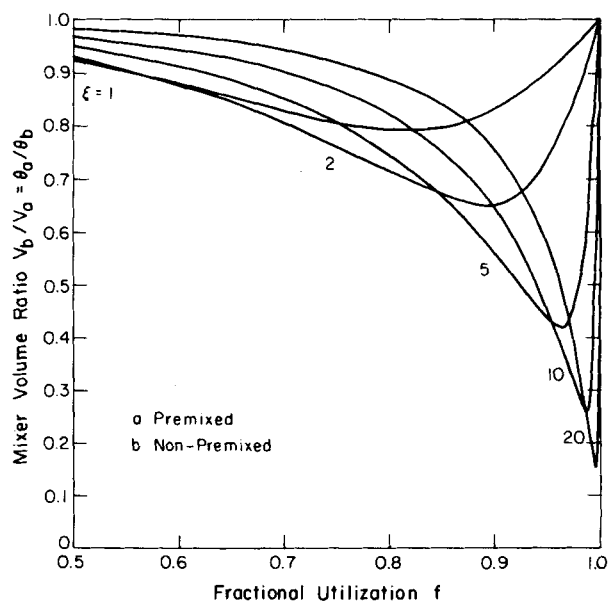


Figure 6. Effect of recycle ratio on relative mixer volumes required for two different emulsion feed and recycle premixing policies.

internal reagent fed to the train as a whole. Our purpose now is to utilize the relations developed above for single-stage operations in the design of multistage LM extraction processes. We consider cocurrent and countercurrent systems separately.

## Cocurrent Operation

For a typical stage  $i$  in a mixer-settler train shown in Figure 7a we can define

$$\theta_i = \frac{c_{IRi-1}}{c_i} \frac{R^2/\alpha D}{V_E/v_E} \quad (34)$$

which, according to our single stage results, is a unique function of the fractional utilization

$$f_i = \frac{v_W}{v_E} \left( \frac{c_{i-1} - c_i}{c_{IRi-1}} \right) \quad (35)$$

for this stage. On eliminating  $c_i$  between these two equations, we can readily show that

$$\gamma_{i-1} = \left( \frac{v_E c_{IRi-1}}{v_W c_{i-1}} \right) = \frac{\theta_i}{\phi + \theta_i f_i} \quad (36)$$

where

$$\phi = \left( \frac{v_W}{v_E} \right) \frac{R^2/\alpha D}{V_E/v_E} = \left( \frac{V_W}{V_E} \right) \frac{R^2/\alpha D}{V_W/v_W} \quad (37)$$

This expression relates the fractional utilization  $f_i$  to the internal reagent and continuous-phase concentrations of the streams fed to the mixer  $i$ , for a specified value of the parameter  $\phi$ . Since  $\theta_i$  and  $f_i$  are related in a unique fashion (for fixed recycle ratio,  $\xi$ ), a set of curves can be prepared giving  $\gamma_{i-1}$  as a function of  $f_i$  (or  $\theta_i$ ) with  $\phi$  as parameter. From these curves, for given values of  $\gamma_{i-1}$  and  $\phi$ , the corresponding fractional utilization  $f_i$  can be determined. This value of  $f_i$  can now be used to determine  $\gamma_i$ , the effluent concentration ratio for stage  $i$ , as is shown below.

The concentration of the internal reagent leaving stage  $i$  can be computed from that of the feed to this stage by the simple balance equation

$$c_{IRi} = (1 - f_i) c_{IRi-1} \quad (38)$$

which can be used to eliminate  $c_{IRi-1}$  from Eq. 34. This leads to

$$\gamma_i = \frac{1}{\phi} (1 - f_i) \theta_i \quad (39)$$

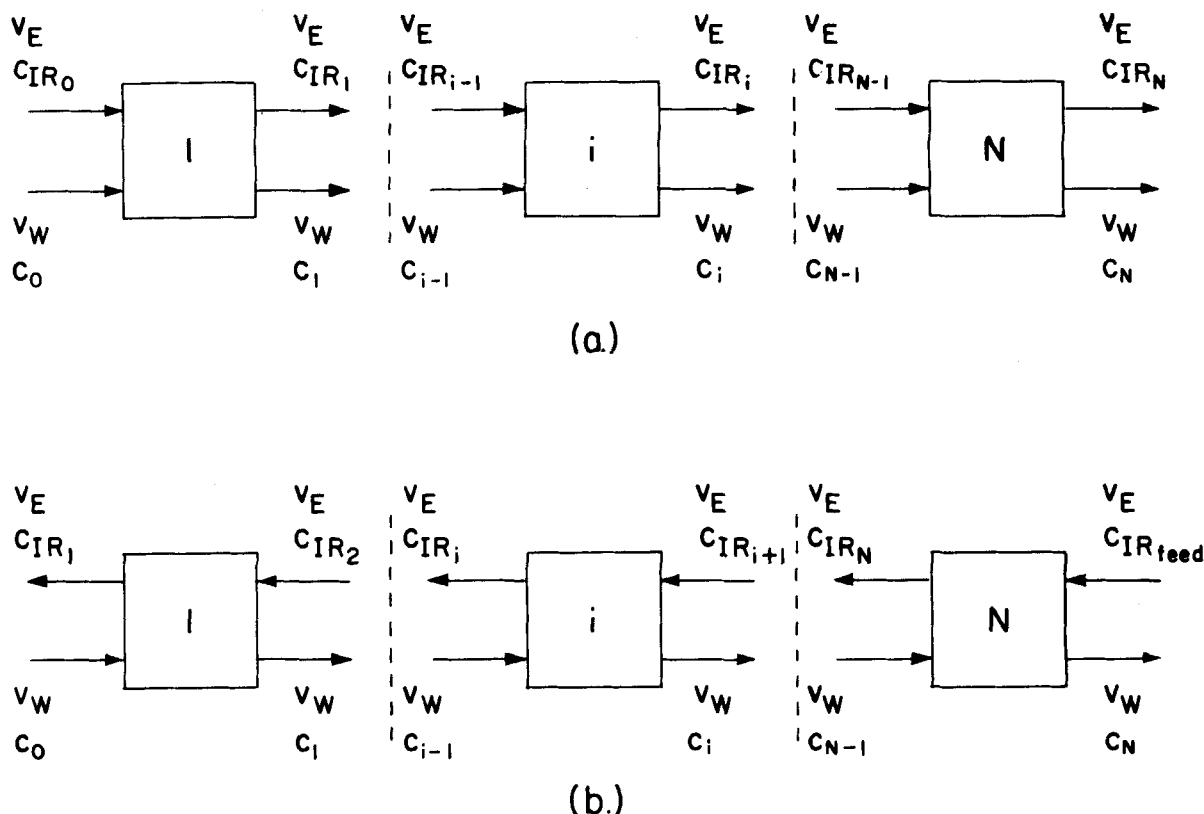


Figure 7. Multistage mixer-settler train: (a) cocurrent (b) countercurrent.

which is again a simple expression for  $\gamma$ , this time for stage  $i$ , in terms of  $f_i$  (or  $\theta_i$ ) and the parameter  $\phi$ . Hence, for a given  $f_i$ ,  $\gamma_i$  can be determined and used with Eq. 36 to estimate  $f_{i+1}$ , and the entire procedure repeated for stage  $i + 1$ . In this manner, starting with the feed condition

$$\gamma_0 = \Gamma = \frac{v_E C_{IR_{feed}}}{v_W C_{feed}}, \quad (40)$$

it is possible to move from stage to stage until the desired effluent concentration levels, corresponding to

$$\frac{\gamma_N}{\Gamma} = \frac{(1 - F)}{(1 - \Gamma F)}, \quad (41)$$

are attained, or until a specified number of stages is reached. In the first case, the number of stages required to effect a given separation is obtained directly, while in the second instance the overall fractional utilization of the internal reagent is estimated using the material balance relation

$$F = \frac{(1 - \gamma_N/\Gamma)}{(1 - \gamma_N)}, \quad (42)$$

This procedure can be carried out graphically, and is also readily implemented for computer calculations. It is entirely analogous to the well-known McCabe-Thiele method for staged equilibrium processes (King, 1980); Eq. 39 plays the role of an equilibrium curve, and Eq. 36 is the effective operating line for the system.

The graphical construction technique outlined above is illustrated in Figure 8, where a constant value of  $\phi = 50$  has been used, and no external recycle has been allowed for (i.e.,  $\xi = 0$ ). The two curves plotted are Eqs. 36 and 39 respectively, and it is immediately evident that these curves intersect at a  $\gamma$ -value of unity. Also, depending on the feed concentration ratio  $\Gamma$ , with increasing stage number  $i$  the values of  $\gamma_i$  can increase ( $\Gamma > 1$ ), decrease ( $\Gamma < 1$ ) or remain unchanged at unity ( $\Gamma = 1$ ). This is because in the presence of a stoichiometric excess of internal reagent ( $\Gamma > 1$ ), a fractional change in the continuous-phase solute concentration does not lead to as large a fractional change in the internal reagent

concentration, and hence  $\gamma_i$  must increase. On the other hand, when  $\Gamma < 1$ , a given decrease in solute concentration brings about a proportionally larger reduction in the internal reagent concentration, culminating in a decrease in the value of  $\gamma_i$  relative to that of  $\gamma_{i-1}$ . For  $\Gamma = 1$ , of course, the solute and internal reagent are fed to the system in stoichiometric proportions, and any decrease in solute concentration is accompanied by a commensurate decrease in internal reagent strength, and the  $\gamma$  values remain unchanged at unity from one stage to the next.

These observations are illustrated clearly in Figure 9, where  $\gamma_N$  has been plotted as a function of the overall fractional utilization  $F$ , with  $\Gamma$  as parameter (Eq. 41). From these curves, it is readily apparent that for  $\Gamma > 1$ , the overall fractional utilization of internal reagent can never increase beyond the value  $1/\Gamma$ , since this corresponds to complete extraction of the solute from the continuous phase. For  $\Gamma < 1$ , however, all values of  $F$  between zero and unity are attainable, although it is no longer possible to remove completely all the solute from the continuous phase. In this case,  $\gamma_N = 0$  for  $F = 1$ .

The graphical or numerical techniques discussed above are not useful when  $\Gamma = 1$ , because then neither  $\gamma_i$  nor  $f_i$  changes from stage to stage. However, for given operating conditions  $\phi$ , a simple analytical expression can be obtained relating  $F$  and  $N$ . From the definition of the overall fractional utilization  $F$ , it follows that

$$(1 - F) = \frac{C_{IR_N}}{C_{IR_0}} = \prod_{i=1}^N \frac{C_{IR_i}}{C_{IR_{i-1}}} = \prod_{i=1}^N (1 - f_i) \quad (43)$$

and thus, when  $f_i$  is a constant ( $f$ , say), independent of stage number  $i$ , we have

$$(1 - F) = (1 - f)^N \quad (\Gamma = 1) \quad (44)$$

or

$$N = \frac{\ln(1 - F)}{\ln(1 - f)} \quad (\Gamma = 1) \quad (45)$$

which gives our desired result. The fractional utilization over each stage,  $f$ , can be related directly to  $\phi$ , and is merely the root of

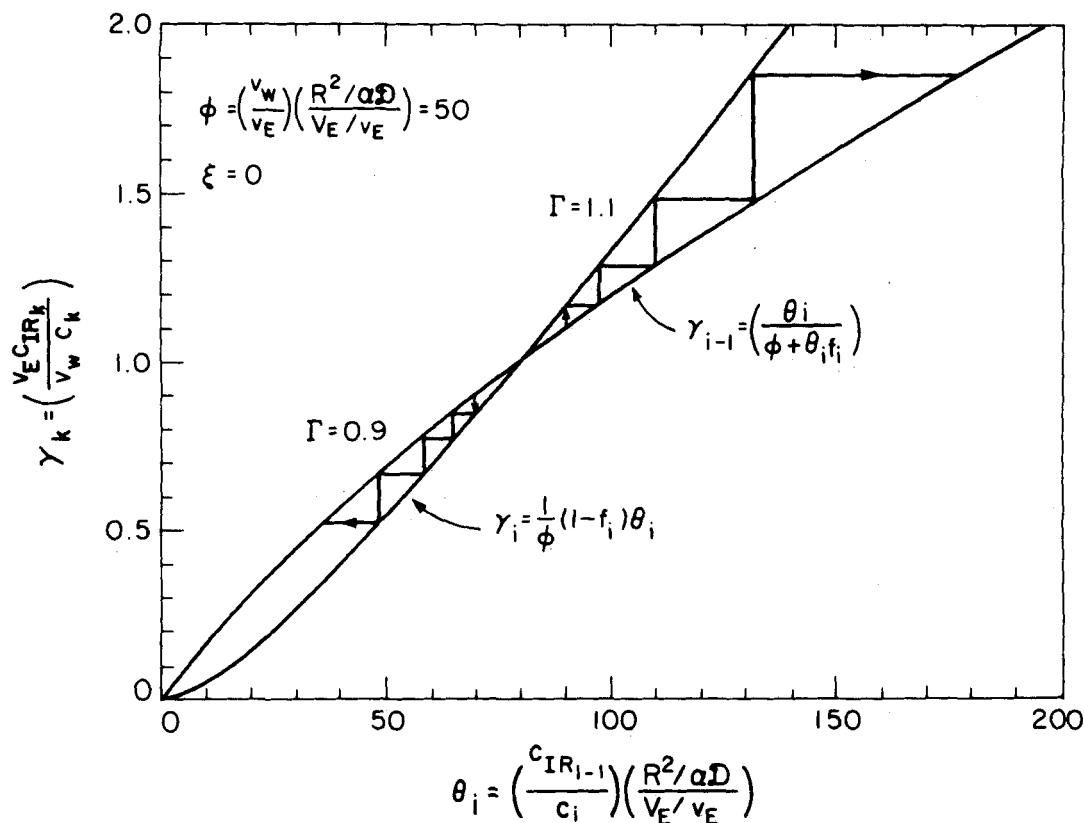


Figure 8. Graphical construction for design of cocurrent, multistage mixer-settler trains.

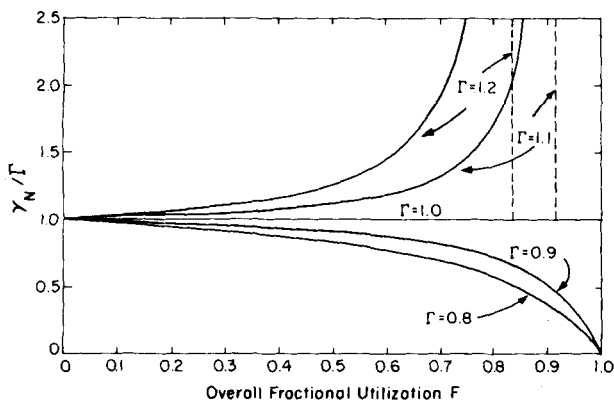


Figure 9. Effect of feed conditions on final concentration ratio,  $\gamma_N$ , in cocurrent operations.

$$(1 - f)\theta = \phi, \quad (46)$$

which equation follows from Eq. 39 with  $\gamma$  set to unity.

While our discussion thus far has assumed constant values for the operating parameters  $\phi$  and  $\xi$  over the entire mixer-settler train, this restriction is not necessary, and, indeed, it is a simple matter to allow for variations in both  $\phi$  and  $\xi$  when going from one stage to the next. Graphically, this requires the construction of a set of curves corresponding to each  $\phi$  and  $\xi$  combination considered, and then ensuring that the correct pair of curves is used for each mixer-settler unit in the sequence.

#### Countercurrent Operation

A procedure analogous to that used above can be developed also for countercurrent operations, with some small changes in the

design equations. Consider the countercurrent mixer-settler system shown in Figure 7b. For stage  $i$  we now have

$$\theta_i = \frac{c_{IRi+1}}{c_i} \frac{R^2/\alpha D}{V_E/v_E} \quad (47)$$

which, on defining

$$\gamma_i = \left(\frac{v_E c_{IRi+1}}{v_w c_i}\right) \quad (48)$$

is seen to be equivalent to the equation

$$\gamma_i = \frac{1}{\phi} \theta_i \quad (49)$$

This, then, relates  $\gamma_i$  to  $\theta_i$  (or  $f_i$ ) uniquely for any given  $\phi$ . The fractional utilization  $f_i$ , is now given by

$$f_i = \frac{v_w}{v_E} \left(\frac{c_{i-1} - c_i}{c_{IRi+1}}\right) \quad (50)$$

We also have

$$c_{IRi} = (1 - f_i)c_{IRi+1} \quad (51)$$

and thus

$$f_i = \frac{v_w}{v_E} \left[ (1 - f_i) \frac{c_{i-1}}{c_{IRi}} - \frac{c_i}{c_{IRi+1}} \right] \quad (52)$$

which can be rearranged to give

$$\gamma_{i-1} = \left(\frac{\theta_i}{\phi + \theta_{fi}}\right) (1 - f_i) \quad (53)$$

note having been taken of the definition (Eq. 48) for  $\gamma$  and the relation (Eq. 49) for  $\gamma_i$ .

Equations 49 and 53 are the counterparts of the equilibrium and material balance equations used in the familiar McCabe-Thiele



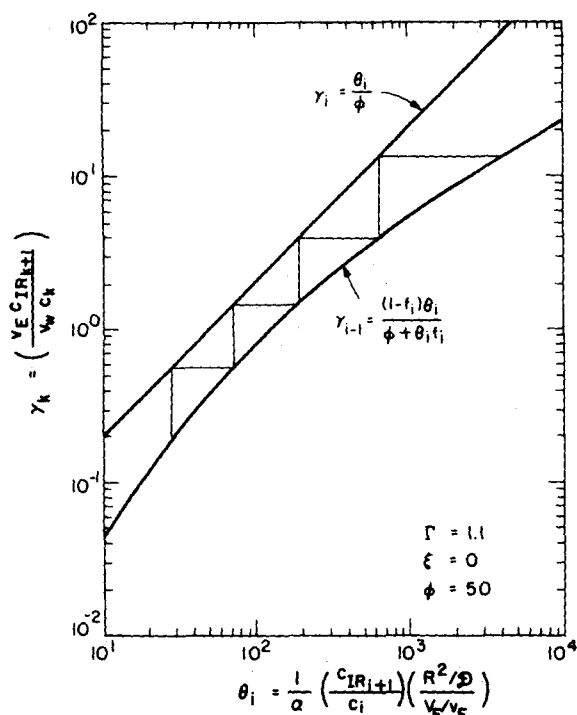


Figure 10. Graphical construction design of countercurrent, multistage mixer-settler trains.

method for equilibrium processes, and can be used in the same way as Eqs. 36 and 39 are used in the graphical or numerical analysis of cocurrent operations. In contrast to the cocurrent case, however, except at  $\gamma = 0$ , the design curves do not intersect. This is evident on Figure 10, where the parameter values  $\phi = 50$  and  $\xi = 0$  have been used in the construction of these curves. Indeed,  $\gamma_i$  will *always* increase with increasing stage number  $i$ , consistent with both an increase in internal reagent concentration and a decrease in continuous-phase solute concentration as  $i$  is incremented.

The design procedure for the countercurrent mixer-settler train is an iterative process. To begin stepping off stages it is necessary to know  $\gamma_o$ , which can be calculated from

$$\gamma_o = \frac{v_E c_{IR1}}{v_W c_o} = (1 - F)\Gamma \quad (54)$$

where we have recognized that  $c_{IR1} = (1 - F)c_{IR\text{feed}}$  and  $c_o \equiv c_{\text{feed}}$ . However,  $F$  itself is unknown at this stage, and an initial guess must be made to obtain  $\gamma_o$ . The accuracy of this initial guess can be checked after the design procedure has been carried out for the desired number of units, and, if correct, it should concur with the value obtained from the material balance equation

$$F = \frac{\gamma_N}{\Gamma} - \frac{\Gamma}{\gamma_N} \quad (55)$$

Generally several iterations on  $F$  are required to ensure convergence.

#### Cocurrent vs. Countercurrent Operations

In the foregoing, we developed procedures for the analysis and design of multistage mixer-settler systems for liquid membrane extraction operations. These procedures are valid whenever the assumptions inherent in the formulation of the Advancing Front Model are upheld. In this section, we use our results to compare the performance of co- and countercurrent mixer-settler configurations for liquid membrane systems which satisfy these requirements.

In most systems of practical interest, the parameter  $\phi$  is expected to be in the range of 10 to 1,000, whereas recycle ratios of between 0 and 20 (and possibly even higher) can be anticipated. Performance curves for multistage mixer-settler extraction operations

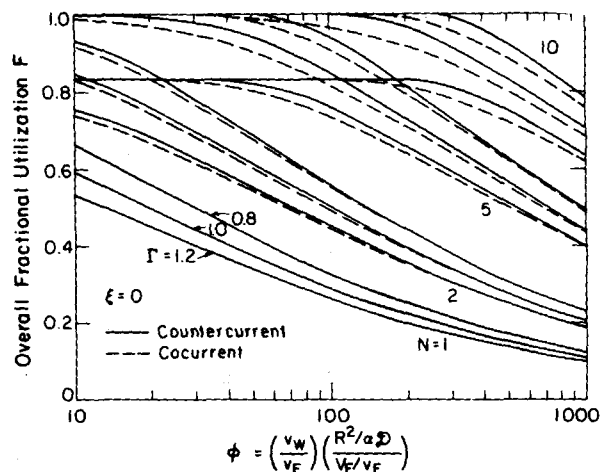


Figure 11. Performance curves for multistage mixer-settler extraction operations using liquid surfactant membranes.

are shown in Figure 11, for the special case of no external recycle, i.e., for  $\xi = 0$ , and covering the relevant range of  $\phi$  values. These curves compare the results obtained for co- and countercurrent operations for a given number,  $N$ , of stages, with the feed condition,  $\Gamma$ , as parameter.

An increase in  $\phi$ , holding  $\Gamma$  and  $N$  constant, is seen to lead to a reduction in the degree of solute extraction from the continuous phase, as reflected in the corresponding decrease in overall fractional utilization of the internal reagent. This result was to be anticipated, since the parameter  $\phi$  is, in essence, the ratio of the diffusional response time,  $R^2/D$ , relative to the emulsion residence time,  $V_E/v_E$ . Thus, for large values of  $\phi$ , the contact time is sufficiently short that the reaction front penetration depth is small, and hence utilization of the internal reagent is low. With increasing contact time (decreasing  $\phi$ ), the penetration of the advancing reaction front into the globule is greater, with a commensurate increase in the utilization of the internal reagent.

The parameter  $\Gamma$  gives the ratio of equivalents of internal reagent fed to the mixer-settler train relative to the equivalents of solute introduced to this train. A  $\Gamma$  value of unity indicates a stoichiometrically-balanced feed condition—for  $\Gamma > 1$  there is an excess of internal reagent, while  $\Gamma < 1$  corresponds to a stoichiometric deficiency of the internal reagent. Consequently, a decrease in fractional utilization of the internal reagent is observed with an increase in the value of  $\Gamma$ , other factors being equal. This does not, however, necessarily reflect a decrease in the *rate* of solute extraction. Indeed, if the increase in  $\Gamma$  is solely due to an increase in  $c_{IR\text{feed}}$ , the rate of solute extraction will also be increased. This is because the rate of penetration of the reaction front, and hence the diffusional resistance to solute transfer, is lower the higher the initial internal reagent concentration, for a given degree of solute extraction. Conversely, if the increase in  $\Gamma$  is due only to a lowering of the solute feed concentration, the rates of mass transfer will be decreased, because then there is a reduced concentration driving force for mass transfer. In either case, the fractional utilization will be less than that obtained for lower values of  $\Gamma$ .

The effect of increasing the number of mixer-settler units in a multistage operation is clearly to increase the overall fractional utilization of the internal reagent. Moreover, it is seen from the results shown in Figure 11 that the difference in performance between the cocurrent and countercurrent configurations becomes more pronounced as the total number of stages is increased. While this is to be expected for equilibrium stage operations, for rate-limited processes it is often found that very little is to be gained by operating in the countercurrent rather than cocurrent mode. Indeed, the model of Cahn and Li (1974) predicts identical behavior for the two cases; however, it ignores the experimentally observed fact that  $D'$  varies with the fractional utilization of internal reagent in any given stage, which in itself is different from stage to stage. In fact, it is this interstage variation in  $f$  that is responsible for the

differences in overall performance of the two contacting arrangements. For cocurrent operation, as one moves from stage to stage, the internal reagent concentration decreases, as does the continuous phase solute concentration. Thus not only does the diffusional resistance increase, but also the concentration driving force for the solute decreases with increasing stage number; both effects act to reduce the overall mass transfer rate. For countercurrent operation, on the other hand, although the solute concentration decreases with increasing stage number, it encounters an emulsion phase increasingly richer in internal reagent, and hence one for which the diffusional resistance becomes increasingly smaller. In this case, the decrease in driving force is counteracted to some extent by the corresponding decrease in diffusional resistance. Thus, countercurrent operation is expected to be, and is, more efficient than cocurrent contacting, as reflected in the numerical results.

The improvement in extraction efficiency gained by using countercurrent rather than cocurrent flow is not as great as one might expect. Even for 5–10 units, the maximum enhancement in the overall fractional utilization of internal reagent is only about 5%. This is because between each stage the emulsion globules are permitted to coalesce, thereby destroying the stagnant film of spent reagent built up during the extraction process—this film provides the primary diffusive resistance to solute permeation into the globules. The interstage settling, therefore, ensures that the resistance to mass transfer developed in a given stage is not cumulative over the entire mixer-settler train. Consequently the inherent advantages of countercurrent *vis-a-vis* cocurrent operations are, to some extent, negated.

The results presented above assume no external recycle over individual stages. The use of a recycle emulsion stream can be taken into account readily as described earlier. In general, an increase in  $\xi$ , with other operating conditions held constant, will result in a higher overall utilization of internal reagent. Also, for all  $\xi$ , the overall fractional utilization can approach unity when  $\Gamma \leq 1$ , but cannot exceed  $1/\Gamma$  for  $\Gamma > 1$ . The former case corresponds to complete utilization of the internal reagent, while for  $\Gamma > 1$  the limiting case refers to the complete removal of the solute to be extracted. These limiting cases obtain only for sufficiently small values of  $\phi$ , and complete depletion of the solute or internal reagent (depending on whether  $\Gamma > 1$  or  $\Gamma < 1$ , respectively) will tend to first occur at higher and higher values of  $\phi$  as  $\xi$  increases.

## DISCUSSION

Many liquid membrane systems obey, at least approximately, the assumptions made in the development of the Advancing Front Model, which has stood the test of experimental verification admirably (Ho et al., 1982; Hatton et al., 1983). In such cases, the procedures outlined above provide an effective design strategy for the scale-up of liquid membrane technology. However, in many other applications the assumption of an irreversible interaction between the solute and the internal reagent cannot be corroborated by the known kinetics of the interaction, and in such cases additional modelling along the lines of that undertaken by Teramoto et al. (1981) is desirable.

Two other factors not accounted for in our modelling approach are the effects of breakage (or leakage) and swell of the membrane emulsions on extraction performance. Breakage effects, in which internal reagent droplets loaded with solute are stripped from the emulsion globules by high shear forces and are assimilated by the agitated external phase, have been described using an extension of the model of Cahn and Li (1974) to include also a first-order loss of extracted solute by breakage (Boyadzhiev et al., 1978; Ho and Li, 1981; Frankenfeld et al., 1981; Terry et al., 1982). It would seem desirable, however, to include in these models also the effect of a distributed and changing resistance to the permeation of the solute. Extension of our current modelling efforts to allow for these effects appears to be feasible, and attention should be devoted to investigation of this approach.

The phenomenon of swell is one for which no mathematical analyses have yet been published. Swell occurs primarily due to the osmotic transport of water from the continuous phase to the encapsulated internal reagent droplets, although it can also occur by direct encapsulation of the continuous phase during the agitation process. This swelling can be detrimental to the overall performance of liquid membrane systems, and it is, therefore, desirable that it be incorporated in future mathematical modelling efforts for the characterization of liquid membrane operations.

## NOTATION

$c$	= continuous-phase solute concentration
$c_o$	= continuous-phase solute concentration in feed
$c_1$	= continuous-phase solute concentration in mixer
$c_g$	= solute concentration in globule (based on volume of emulsion)
$c_{IR}$	= internal reagent concentration (based on volume of emulsion)
$D'$	= permeation rate constant
$D$	= effective solute diffusivity in emulsion
$F$	= overall fractional utilization of internal reagent
$f$	= fractional utilization of internal reagent over a single mixer-settler stage
$g$	= dimensionless solute concentration in globule = $c_g/\alpha c_1$
$N$	= number of stages in a mixer-settler train
$N_T$	= total number of globules in mixer
$n(t)$	= fraction of globules having residence time greater than $t$
$R$	= globule radius
$R_f$	= reaction front position
$r$	= radial coordinate
$r_o$	= solute extraction rate
$T$	= average emulsion residence time in mixer
$t$	= residence time
$V_E$	= emulsion phase holdup volume in mixer
$V_W$	= continuous phase holdup volume in mixer
$V_M$	= mixer volume
$v_E$	= emulsion phase volumetric flow rate
$v_W$	= continuous phase volumetric flow rate

## Greek Letters

$\alpha$	= partition coefficient for solute between external phase and emulsion
$\Gamma$	= feed concentration ratio = $v_E c_{IR_{feed}}/v_W c_{feed}$
$\gamma_i$	= concentration ratio = $(v_E c_{IR_i}/v_W c_i)$ for cocurrent, $(v_E c_{IR_{i+1}}/v_W c_i)$ for countercurrent
$\epsilon$	= perturbation parameter = $\alpha c_1/c_{IR}$
$\eta$	= dimensionless radial coordinate = $r/R$
$\theta$	= parameter in Advancing Front Model defined by Eq. 22
$\xi$	= external emulsion recycle ratio
$\tau$	= dimensionless time = $\epsilon D t/R^2$
$\phi$	= parameter in Advancing Front Model defined by Eq. 37
$\phi_e$	= holdup ratio = $V_E/V_W$
$\chi$	= dimensionless reaction front position = $R_f/R$

## LITERATURE CITED

- Alessi, P., I. Kikic, and M. Orlandini-Visalberghi, "Liquid Membrane Permeation for the Separation of  $C_8$  Hydrocarbons," *Chem. Eng. J.*, **19**, 221 (1980).
- Asher, W. J., et al., "Liquid Membrane System Directed toward Chronic Uremia," *Kidney Int.*, **7**, S-409 (1975).
- Asher, W. J., et al., "Liquid Membrane Capsules for Chronic Uremia," *Trans. Am. Soc. Artif. Intern. Organs*, **23**, 673 (1977).
- Bock, J., R. R. Klein, P. L. Valint, and W. S. Ho, "Liquid Membrane Extraction of Uranium from Wet Process Phosphoric Acid—Field Process

- Demonstration," Paper No. 30b, AIChE Annual Meeting, New Orleans, LA (Nov. 8-12, 1981).
- Bock, J., and P. L. Valint, "Uranium Extraction from Wet Process Phosphoric Acid. A Liquid Membrane Approach," *Ind. Eng. Chem. Fund.*, **21**, 417 (1982).
- Boyadzhiev, L., T. Sapundzhiev, and E. Bezenshek, "Modelling of Carrier-Mediated Extraction," *Sep. Sci.*, **12**, 541 (1978).
- Cahn, R. P., and N. N. Li, "Separation of Phenol from Waste Water by the Liquid Membrane Technique," *Sep. Sci.*, **9**, 505 (1974).
- Cahn, R. P., and N. N. Li, "Separations of Organic Compounds by Liquid Membrane Process," *J. Membrane Sci.*, **1**, 129 (1976a).
- Cahn, R. P., and N. N. Li, "Hydrocarbon Separation by Liquid Membrane Processes," *Membrane Separation Processes*, P. Meares, Ed., Ch. 9, 327, Elsevier Scientific Publishing Co., Amsterdam-New York (1976b).
- Cahn, R. P., N. N. Li, and R. M. Minday, "Removal of Ammonium Sulfide from Wastewater by Liquid Membrane Processes," *Environ. Sci. Tech.*, **12**, 1051 (1978).
- Frankenfeld, J. W., and N. N. Li, "Waste Water Treatment by Liquid Ion Exchange in Liquid Membrane Systems," *Recent Developments in Separation Science*, N. N. Li, Ed., **3**, 285, Chemical Rubber Co., Cleveland, OH (1977).
- Frankenfeld, J. W., W. J. Asher, and N. N. Li, "Biochemical and Biomedical Separations Using Liquid Membranes," *Recent Developments in Separation Science*, N. N. Li, Ed., **4**, 39, Chemical Rubber Co., Cleveland, OH (1978).
- Frankenfeld, J. W., R. P. Cahn, and N. N. Li, "Extraction of Copper by Liquid Membranes," *Sep. Sci. Tech.*, **16**, 385 (1981).
- Halwachs, W., E. Flaschel, and K. Schügerl, "Liquid Membrane Transport—A Highly Selective Separation Process for Organic Solutes," *J. Membrane Sci.*, **6**, 33 (1980).
- Hatton, T. A., E. N. Lightfoot, and N. N. Li, "The Mathematical Modelling of Liquid Surfactant Membranes," *Proc. Joint CIESC/AIChE Meeting*, Beijing, China, 558 (Sept., 1982).
- Hatton, T. A., E. N. Lightfoot, R. P. Cahn, and N. N. Li, "An Internal Recycle Mixer for Solvent Extraction. Mass Transfer Characterization with Liquid Surfactant Membranes," *Ind. Eng. Chem. Fund.*, **22**, 27 (1983).
- Hayworth, H. C., W. S. Ho, W. A. Burns, and N. N. Li, "Extraction of Uranium from Wet Process Phosphoric Acid by Liquid Membranes," Paper No. 56d, AIChE Nat. Meeting, Orlando, FL (Feb. 28-Mar. 3, 1982).
- Ho, W. S., and N. N. Li, "Modelling of Liquid Membrane Extraction," Paper No. 89, ACS Nat. Meeting, New York (Aug. 23-28, 1981).
- Ho, W. S., T. A. Hatton, E. N. Lightfoot, and N. N. Li, "Batch Extraction with Liquid Surfactant Membranes: A Diffusion Controlled Model," *AIChE J.*, **28**, 662 (1982).
- Hochhauser, A. M., and E. L. Cussler, "Concentrating Chromium with Liquid Surfactant Membranes," *AIChE Symp. Ser.*, **71**, 136 (1975).
- King, C. J., *Separation Processes*, 2nd Ed., McGraw-Hill, New York (1980).
- Kitagawa, T., Y. Nishikawa, J. W. Frankenfeld, and N. N. Li, "Wastewater Treatment by Liquid Membrane Process," *Environ. Sci. Technol.*, **11**, 602 (1977).
- Kondo, K., et al., "Extraction of Copper with Liquid Surfactant Membranes Containing Benzoylacetone," *J. Chem. Eng. Japan.*, **12**, 203 (1979).
- Kondo, K., K. Kita, and F. Nakashio, "Extraction Kinetics of Copper with Liquid Surfactant Membranes in a Stirred Transfer Cell," *J. Chem. Eng. Japan.*, **14**, 20 (1981).
- Kopp, A. G., R. J. Marr, and F. E. Moser, "A New Concept for Mass Transfer in Liquid Surfactant Membranes without Carriers and with Carriers that Pump," *Instn. Chem. Eng. Symp. Ser.*, **54**, 279 (1978).
- Kremesec, V. J., and J. C. Slatery, "Analysis of Batch, Dispersed-Emulsion, Separation Systems," *AIChE J.*, **28**, 492 (1982).
- Li, N. N., "Permeation through Liquid Surfactant Membranes," *AIChE J.*, **17**, 459 (1971a).
- Li, N. N., "Separation of Hydrocarbons by Liquid Membrane Permeation," *Ind. Eng. Chem. Process Des. Dev.*, **10**, 215 (1971b).
- Li, N. N., and A. L. Shrier, "Liquid Membrane Water Treating," *Recent Dev. in Sep. Sci.*, N. N. Li, Ed., **1**, 163, Chemical Rubber Co., Cleveland, Ohio (1972).
- Li, N. N., and W. J. Asher, "Blood Oxygenation by Liquid Membrane Permeation," *Chem. Eng. in Med.*, ACS (Advances in Chemistry Series), **1** (1973).
- Martin, T. P., and G. A. Davies, "The Extraction of Copper from Dilute Aqueous Solutions Using a Liquid Membrane Process," *Hydrometallurgy*, **2**, 315 (1976/1977).
- Matulevicius, E. S., and N. N. Li, "Facilitated Transport through Liquid Membranes," *Sep. Purif. Methods*, **4**, 73 (1975).
- May, S. W., and N. N. Li, "The Immobilization of Urease Using Liquid-Surfactant Membranes," *Biochem. Biophys. Res. Commun.*, **47**, 1179 (1972).
- May, S. W., and N. N. Li, "Encapsulation of Enzymes in Liquid Membrane Emulsions," *Enzyme Engineering*, E. K. Pye and L. B. Wingard, Eds., **1**, 77, Plenum Press, New York (1974).
- May, S. W., and N. N. Li, "Liquid-Membrane-Encapsulated Enzymes," *Biomed. Appl. of Immobilized Enzymes and Proteins*, T. M. S. Chang, Ed., **1**, 171, Plenum Press, New York (1977).
- Mohan, R. R., and N. N. Li, "Reductions and Separations of Nitrate and Nitrite by Liquid Membrane-Encapsulated Enzymes," *Biotechnol. Bioeng.*, **16**, 513 (1974).
- Mohan, R. R., and N. N. Li, "Nitrate and Nitrite Reduction by Liquid Membrane-Encapsulated Whole Cells," *ibid.*, **17**, 1137 (1975).
- Pedroso, R. I., and G. A. Domoto, "Perturbation Solutions for Spherical Solidification of Saturated Liquids," *Trans. ASME J. Heat Transfer*, **95**, 42 (1973).
- Schiffer, D. K., A. Hochhauser, D. F. Evans, and E. L. Cussler, "Concentrating Solutes with Membranes Containing Carriers," *Nature*, **250**, 484 (1974).
- Schlosser, S., and E. Kossackzy, "Comparison of Pertraction Through Liquid Membranes and Double Liquid-Liquid Extraction," *J. Membrane Sci.*, **6**, 83 (1980).
- Shah, N. D., and T. C. Owens, "Separation of Benzene and Hexane with Liquid Membrane Technique," *Ind. Eng. Chem. Prod. Res. Dev.*, **11**, 58 (1972).
- Strelzicki, J., and W. Charewicz, "The Liquid Surfactant Membrane Separation of Copper, Cobalt and Nickel from Multicomponent Aqueous Solutions," *Hydrometallurgy*, **5**, 243 (1980).
- Teramoto, M., et al., "Extraction of Amine by W/O/W Emulsion System," *J. Chem. Eng. Japan*, **14**, 122 (1981).
- Terry, R. E., N. N. Li, and W. S. Ho, "Extraction of Phenolic Compounds and Organic Acids by Liquid Membranes," *J. Membrane Sci.*, **10**, 305 (1982).
- Völkel, W., W. Halwachs, and K. Schügerl, "Copper Extraction by Means of a Liquid Surfactant Membrane Process," *J. Membrane Sci.*, **6**, 19 (1980).

Manuscript received January 3, 1983; revision received July 18, and accepted August 21, 1983.